Rossby Wave Phase Speed Influences Heatwave Location through a Shift in Storm Track Position

Wolfgang Wicker[1], Nili Harnik[2], Maria Pyrina[3], and Daniela I.V. Domeisen[3]

[1]University of Lausanne
[2]Tel Aviv University
[3]ETH Zurich

January 13, 2024

Abstract

Surface anticyclones connected to the ridge of an upper-tropospheric Rossby wave are the dynamical drivers of mid-latitude summer heatwaves. It is, however, unclear to which extent an anomalously low zonal phase speed of the wave in the upper troposphere is necessary for persistent temperature extremes at the surface. Here, we use spectral analysis to estimate a categorical phase speed for synoptic-scale waves. A composite analysis of ERA5 reanalysis data reveals how a meridional shift in the Rossby wave packet envelope associated with a change in phase speed alters the geographically phase-locked stationary wave pattern. In both composites for amplified low or high phase speed waves, respectively, the ridges and troughs of these temporal-mean wave trains show enhanced and reduced heatwave frequency. The phase speed of synoptic-scale waves is, hence, crucial for where, but less important for whether heatwaves occur.

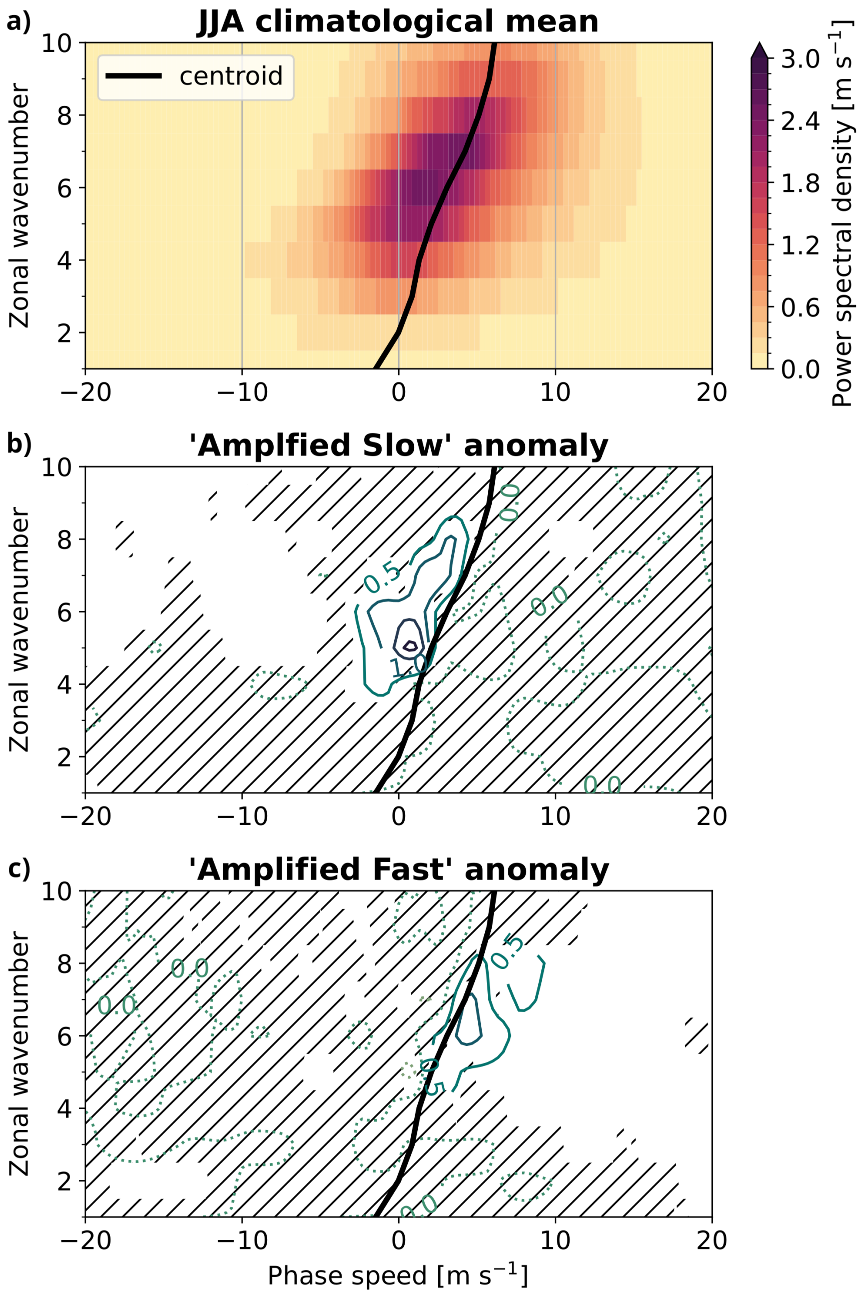
a)
JJA climatological mean
centroid
Zonal wavenumber
Power spectral density [m s^{-1}]
b)
'Amplfied Slow' anomaly
Zonal wavenumber
c)
'Amplified Fast' anomaly
Zonal wavenumber
Phase speed [m s^{-1}]

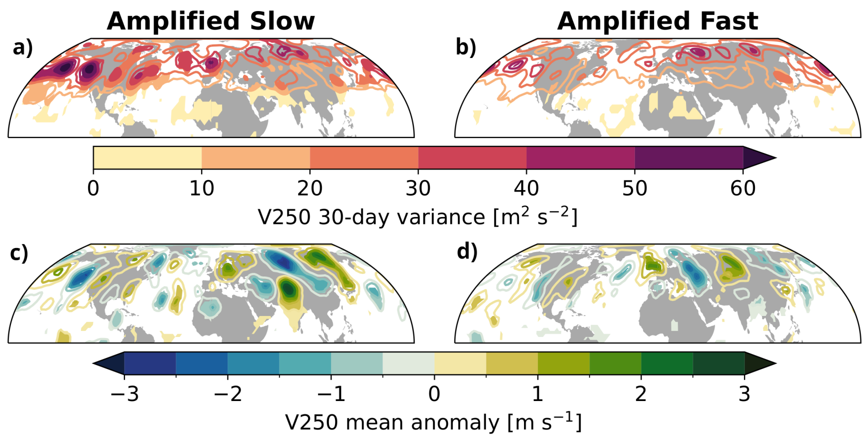
Amplified Slow
Amplified Fast
a)
b)
0
10
20
30
40
50
60
V250 30-day variance [m^2 s^{-2}]
c)
d)
−3
−2
−1
0
1
2
3
V250 mean anomaly [m s^{-1}]

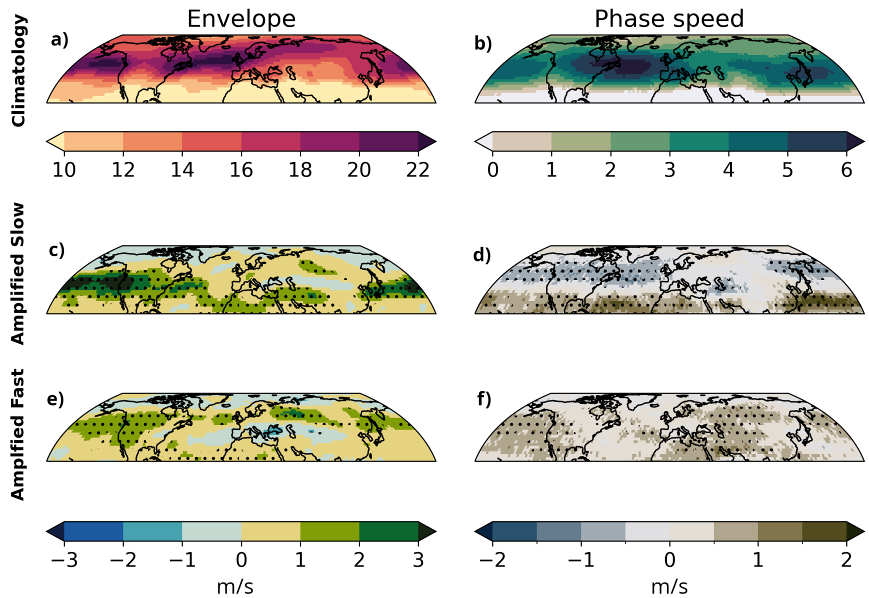
Envelope
Phase speed
Climatology
a)
b)
10
12
14
16
18
20
22
0
1
2
3
4
5
6
Amplified Slow
c)
d)
Amplfied Fast
e)
f)
−3
−2
−1
0
1
2
3
m/s
−2
−1
0
1
2
m/s

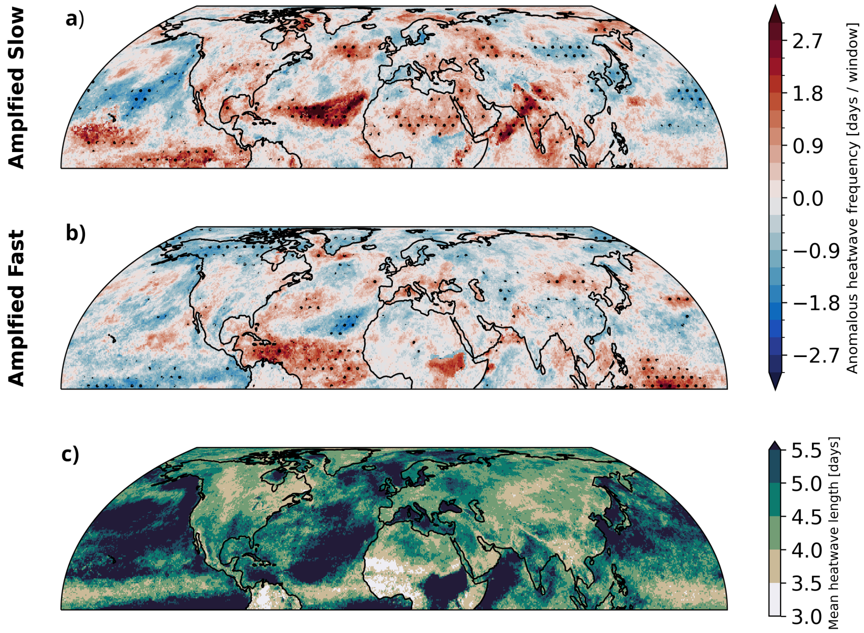
a)
Amplfied Slow
b)
Amplfied Fast
c)
2.7
1.8
0.9
0.0
−0.9
−1.8
−2.7
Anomalous heatwave frequency [days / window]
5.5
5.0
4.5
4.0
3.5
3.0
Mean heatwave length [days]

Rossby Wave Phase Speed Influences Heatwave Location through a Shift in Storm Track Position

Wolfgang Wicker[1], Nili Harnik[2], Maria Pyrina[3], Daniela I. V. Domeisen[1,3]

[1]Faculty of Geosciences and Environment, University of Lausanne, Lausanne, Switzerland
[2]Porter School of the Environment and Earth Sciences, Tel Aviv University, Tel Aviv, Israel
[3]Department of Environmental Systems Science, ETH Zurich, Zurich, Switzerland

Key Points:

- Synoptic-scale wave phase speed is a function of the latitudinal storm track position.
- Phase speed determines where heatwaves occur by shaping temporal-mean circulation anomalies.
- Mean anticyclonic flow in the upper-troposphere is more important for the number of heatwave days than the mean heatwave duration.

Corresponding author: Wolfgang Wicker, `wolfgang.wicker@unil.ch`

Abstract

Surface anticyclones connected to the ridge of an upper-tropospheric Rossby wave are the dynamical drivers of mid-latitude summer heatwaves. It is, however, unclear to which extent an anomalously low zonal phase speed of the wave in the upper troposphere is necessary for persistent temperature extremes at the surface. Here, we use spectral analysis to estimate a categorical phase speed for synoptic-scale waves. A composite analysis of ERA5 reanalysis data reveals how a meridional shift in the Rossby wave packet envelope associated with a change in phase speed alters the geographically phase-locked stationary wave pattern. In both composites for amplified low or high phase speed waves, respectively, the ridges and troughs of these temporal-mean wave trains show enhanced and reduced heatwave frequency. The phase speed of synoptic-scale waves is, hence, crucial for where, but less important for whether heatwaves occur.

Plain Language Summary

High pressure systems tend to be associated with mid-latitude summer heatwaves, defined as multiple consecutive hot days. The persistence criterion in the heatwave definition raises the question whether the associated high pressure system has to be anomalously persistent as well. Using a combination of observational data and atmospheric model output that is commonly regarded as ground truth for prediction purposes we find that this is not the case. By re-distributing the location of on-average high air pressure, some regions experience an increased heatwave frequency even if the atmospheric circulation is less persistent than usual. Understanding the link between persistent surface temperature extremes and the atmospheric circulation is important for the prediction and projection of extreme events in a warming climate.

1 Introduction

The increased frequency in hot temperature extremes is a direct consequence of anthropogenic climate change (Meehl & Tebaldi, 2004; Coumou et al., 2013; Fischer & Knutti, 2015; S. Russo et al., 2015; E. Russo & Domeisen, 2023). Surface heat extremes that last several days, commonly referred to as heatwaves, adversely impact morbidity and can cause excess mortality (e.g., Ebi et al., 2021). Adaptation to and prediction of such extreme events, hence, requires a better understanding of heatwave drivers (Domeisen et al., 2023). The increase in heatwave frequency due to climate change is at least partly driven by thermodynamic feedbacks with the land surface involving latent and sensible heat fluxes (Fischer et al., 2007; Miralles et al., 2014; Hauser et al., 2016). On the other hand, it remains unclear whether or to what extent atmospheric dynamics contribute to the more frequent temperature extremes under climate change. Anticyclonic circulation anomalies in the upper troposphere provide a necessary ingredient for mid-latitude summer heatwaves (Schneidereit et al., 2012; Pfahl & Wernli, 2012; Sousa et al., 2018) and, in particular, synoptic-scale waves with zonal wavenumbers in the range of 6-8 have been identified as dynamical heatwave drivers (Kornhuber et al., 2019; Di Capua et al., 2021). A focus is often set on slow-moving anticyclones or stationary waves (Jiménez-Esteve & Domeisen, 2022; Jiménez-Esteve et al., 2022).

In mid-latitudes, synoptic-scale disturbances are usually associated with the fastest-growing mode of moist baroclinic instability and marked as transient waves by an eastward phase propagation. Petoukhov et al. (2013), on the other hand, proposed a mechanism termed *quasi-resonant amplification* to explain the occurrence of amplified stationary synoptic-scale waves, using a monochromatic wave ansatz that expresses a circumglobal wave train with zero frequency. By deducing characteristics of the wave from properties of the zonal-mean state, this mechanism projects an increase in persistent weather extremes in a warmer climate, based solely on dry dynamics without thermodynamic feedbacks, with a strong and narrow jet creating an efficient waveguide (Mann et al., 2017). However, the applicability of the underlying theory such as *WKBJ* ray tracing techniques has been questioned, calling for an improved definition of waveguidability (Wirth, 2020; Wirth & Polster, 2021; White et al., 2022).

Instead of monochromatic normal modes that are used to develop the quasi-resonant amplification mechanism, metrics of regional jet waviness (Röthlisberger et al., 2016) or the amplitude of localized Rossby wave packets (Fragkoulidis et al., 2018) constitute an alternative representation of the anticyclone that generates a heatwave. A range of typical mid-latitude processes governs the evolution of Rossby wave packets, i.e., cyclogenesis, downstream development, and wave breaking (e.g., Wirth et al., 2018). The energy propagation of localized wave packets can be expressed by a spatial group velocity vector field. The case in which the energy propagation is faster than the phase propagation is termed *downstream development* and can be readily understood for barotropic waves via the Rossby wave dispersion relation (Rossby, 1945; Yeh, 1949). For baroclinic waves, on the other hand, vortex stretching can produce new circulation extremes both downstream and upstream of the original disturbance (Simmons & Hoskins, 1979). Recurrent Rossby wave packets where troughs and ridges repeatedly amplify in the same location can be particularly impactful for weather extremes such as heatwaves, cold spells, floods, and droughts (Zschenderlein et al., 2018; Röthlisberger et al., 2019; Ali et al., 2021).

It seems fair to assume that the persistence of near-surface temperatures inherent to the heatwave definition requires a similarly persistent atmospheric circulation, although it is not clear whether this notion of atmospheric persistence should apply only regionally, or for the state of the entire hemisphere as suggested by the stationary circumglobal wave train perspective (Petoukhov et al., 2013; Mann et al., 2017; Kornhuber et al., 2019; Di Capua et al., 2021). Rossby wave phase speed is a manifest measure of atmospheric persistence and has indeed been connected with mid-latitude temperature extremes (Riboldi et al., 2020). However, the phase speed metric by Riboldi et al. (2020) is a weighted estimate for zonal wavenumbers 1-15 and the reported linkage between phase speed and heatwaves has to be interpreted bearing in mind the clear relationship between phase speed and wavenumber from linear theory. We develop a categorical phase speed estimate of *"amplified slow"* versus *"amplified fast"* defining the range of low and high phase speeds for each wavenumber individually and focusing on zonal wavenumbers 5-8 (see Sec. 2.1). Based on this categorical estimate, we then present a composite analysis of upper-tropospheric low-frequency variability, Rossby wave packet diagnostics, and heatwave frequency for episodes of low and high phase speed, respectively.

2 Data and Methods

In this study, we conduct a statistical analysis of ERA5 reanalysis data (Hersbach et al., 2020) for boreal summer (June-August, JJA) for the period 1959-2021. The backward extension of the ERA5 set grants a larger sample size but renders a temperature detrending necessary for heatwave diagnosis to account for anthropogenic climate change (see Sec. 2.2). For convenience, the pressure level data is downsampled to the horizontal resolution of a $2^{\circ} \times 2^{\circ}$ regular grid and 6-hourly temporal resolution which is sufficient for an accurate estimation of synoptic-scale wave phase speed (see Sec. 2.1). For the heatwave diagnosis, we use daily maximum 2m temperature computed from 1-hourly resolution data on a $0.5^{\circ} \times 0.5^{\circ}$ regular grid.

2.1 Categorical Phase Speed Estimate

In order to diagnose upper-tropospheric Rossby wave phase speed, we compute Hayashi spectra (Hayashi, 1979) of meridional wind anomalies at every grid point on the 250hPa surface between 35°N-65°N following the methodology of Randel and Held (1991). This involves a two-dimensional Fourier transformation of gridded meridional wind anomalies defined with respect to the local climatology at each grid point. Power spectral density is then averaged meridionally in coordinates of zonal wavenumber and phase speed (see the supporting information for technical details). Prior to the spectral analysis, the time series of meridional wind is divided into 30-day windows with a Hanning window taper and 50% overlap to obtain a time series of phase speed spectra. The largest detectable phase speed associated with the Nyquist frequency and the phase speed resolution of the spectral analysis depend both on zonal wavenumber and latitude. For the 6-hourly time resolution and 30-day window length, we obtain a maximum phase speed of 85 ms^{-1} and a phase speed resolution of 1.4 ms^{-1} for wavenumber 7 at 50°N, for example. The non-zero temporal mean anomaly of individual 30-day windows used as input for the spectral analysis is identified as a zero-phase speed wave.

Since the goal of this study is to analyze the role of phase speed on temperature extremes, the continuous phase speed spectrum is divided into a *"slow"* and a *"fast"* phase speed bin for each wavenumber individually at the respective centroid of the JJA climatological-mean Hayashi spectrum (Fig. 1). Composites of power spectral density, meridional wind, heatwave frequency and Rossby wave packets are constructed by selecting 30-day episodes based on a 90th percentile threshold criterion for integrated meridional wind variance in the respective phase speed bin. Specifically, the meridional wind variance is summed for zonal wavenumbers $k = 5, ..., 8$ to focus on synoptic-scale variability. This way, either composite, "amplified slow" or "amplified fast", is composed of 31 windows distributed over 23 and 25 years, respectively, without a clustering at one end of the time series indicative of a trend. There is, however, a dependence on the seasonal cycle with more "amplified slow" occurrences in early than in late summer, and fewer "amplified fast" estimates in central summer than at the margins. The significance of composite means and composite variances is estimated using a parametric bootstrap similar to a Student's t-test and F-test, respectively.

2.2 Rossby Wave Packet and Heatwave Diagnostics

In addition to 30-day mean upper-tropospheric wind anomalies, Rossby wave packet and heatwave diagnostics provide means for analysing intra-composite variability at a higher temporal resolution, 6-hourly and daily, respectively. The envelope and phase of a Rossby wave packet can be calculated as the absolute value and argument of the complex-valued Hilbert transform of 6-hourly meridional wind anomalies (Zimin et al., 2003). The local phase speed is estimated using finite differences in time and longitude provided that the envelope surpasses a threshold of 15 ms^{-1} (Fragkoulidis & Wirth, 2020).

The heatwave detection algorithm is based on daily maximum temperatures at 2 m height that are detrended by regressing the local time series on the time series of 9-year lowpass filtered global-mean surface air temperature to account for the strong thermodynamic trend in the reanalysis data. Heatwave days are then defined as the exceedances of the 90th percentile of the local empirical probability distribution of detrended surface air temperatures lasting for at least three consecutive days (e.g., S. Russo et al., 2015).

3 Results from Composite Analysis

The JJA climatological-mean Hayashi spectrum for upper-tropospheric meridional wind in the Northern hemisphere mid-latitudes shows maximum power spectral density for zonal wavenumbers 5 to 8 (Fig. 1a). From baroclinic Rossby wave dynamics and recent studies of upper-tropospheric Hayashi spectra (e.g., Jiménez-Esteve et al., 2022), we expect an increasing phase speed with increasing zonal wavenumber. This expectation is confirmed by Figure 1. While long waves (wavenumbers 2-4) show a phase speed distribution nearly symmetric around zero and can be considered stationary, shorter wavelengths (wavenumber 6-9) are predominantly eastward propagating, as indicated by the centroid of the phase speed distribution (solid black line in Fig. 1).

Properties of the categorical phase speed estimate "amplified slow" versus "amplified fast" as defined in Section 2.1 are illustrated as composite-mean power spectral density anomalies (Fig. 1b, c). For both categories, spectral power is enhanced in the respective phase speed bin without significantly altering spectral power in the opposing phase speed bin. In other words, the "amplified slow" composite-mean anomaly is roughly centered around a phase speed of 0 ms^{-1}, whereas the "amplified fast" composite indicates pronounced eastward phase propagation on the order of 5 ms^{-1}. The independence of composites seen in power spectral density anomalies is a result of tuning the spectral analysis, i.e., the choice of a 30-day window as explained in the supplementary material, and ensures that the signal of high-phase speed waves is not simply caused by the absence of low-phase speed waves. On the other hand, composite-mean anomalies of power spectral density are largest in proximity to the centroid of the climatological-mean phase speed distribution. Hence, there is no clear indication of a bimodal phase speed behaviour which could provide a natural choice for separating the two phase speed bins. Choosing the centroid of the climatological mean spectrum ensures approximately equal variance in either phase speed bin, both in the climatological mean and the composite-mean anomaly.

Particularly impactful summer heatwaves are found to be associated with multi-week or monthly-mean circulation anomalies in the mid- or upper troposphere (e.g., García-Herrera et al., 2010; Schneidereit et al., 2012; Kornhuber et al., 2019; Yiou et al., 2020), commonly interpreted as the signature of stationary waves. To systematically assess the importance of phase speed for creating temporal-mean wave structures, we conduct a composite analysis of 30-day mean meridional wind anomalies at 250hPa based on our categorical phase speed estimate (Fig. 2). Given the composite-mean power spectral density anomalies in Figure 1, we expect enhanced low-frequency variability or stationary wave power in the "amplified slow" composite. This expectation is confirmed by the composite variance of 30-day mean anomalies with a statistically significantly enhanced variance compared to climatology from the mid-latitude Pacific across North America to the Atlantic (Fig. 2a). The low-frequency variability in the "amplified fast" composite, on the other hand, is not significantly different from climatology (Fig. 2b).

A less expected picture is drawn by the composite-mean anomalies, which show significant values of similar magnitude for both composites, throughout the mid-latitudes but especially over the Eurasian continent (Fig. 2c, d). Interestingly, the "amplified slow" composite highlights a mode with higher meridional wavenumber than the "amplified fast" case. The crucial difference between the composite-mean signal and the composite variance is that the weak stationary wave in the composite mean has a significant longitudinal phase preference and can be described as geographically phase-locked. Without such phase preference, any stationary wave contributes to the composite variance, not the composite mean. We note in particular that finding a significant composite-mean signal for episodes with amplified high phase speed waves does not agree with a normal

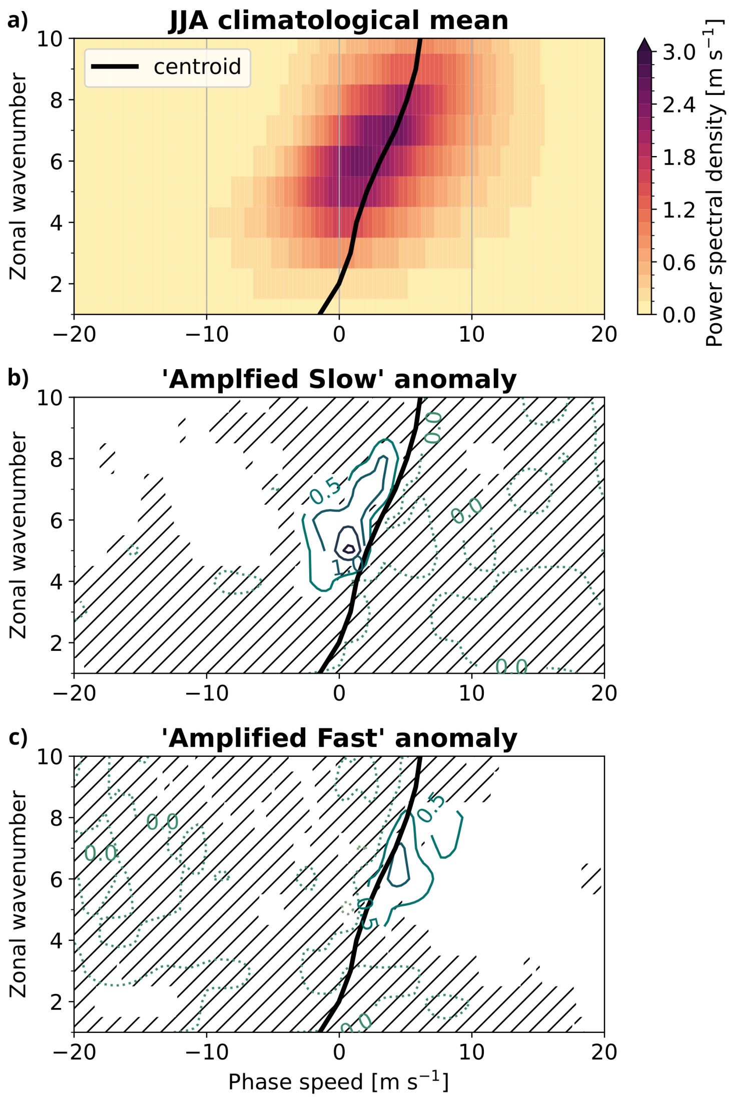

Figure 1. Meridional-mean (35°N-65°N) power spectral density of meridional wind at 250hPa. The solid black line indicates the centroid of the climatological mean spectrum separating the 'slow' and 'fast' phase speed bins. Hatching in panel b and c indicates where episodes with meridional wind variance exceeding the 90th percentile in the respective phase speed bin do not produce a statistically significant composite-mean anomaly at the 95% confidence level.

mode wave ansatz of constant wave amplitude in longitude and time where the eastward phase propagation would efface any composite mean different from zero. The mean signal can, however, be explained by localized Rossby wave packets, downstream development, or recurrent cyclogenesis (e.g., Wirth et al., 2018; Röthlisberger et al., 2019). As long as the wave energy in one location is intermittent and the timing of significant energy is synchronised with the phase of the wave, rapid phase propagation does not efface the temporal-mean signal.

As explained in Section 2.1, the composite analysis in Figure 2 is based on a criterion for meridional wind variance aggregated over the range of wavenumbers 5-8. The results are qualitatively similar when focusing on individual wavenumbers (see Fig. S2). More specifically, the mean anomaly for the composites based on the wavenumber range is close to the sum of composite-mean anomalies for individual wavenumbers. Also note that, since the upper-tropospheric wind is, to first order, horizontally non-divergent, an anomalous meridional wind also requires composite-mean zonal wind anomalies (Fig. S3a, b). In addition to the strong wavy component of the zonal wind anomalies, the zonal-mean zonal wind shows a southward shift for the "amplified slow" composite and a widening of the climatological jet for the "amplified fast" composite (Fig. S3c).

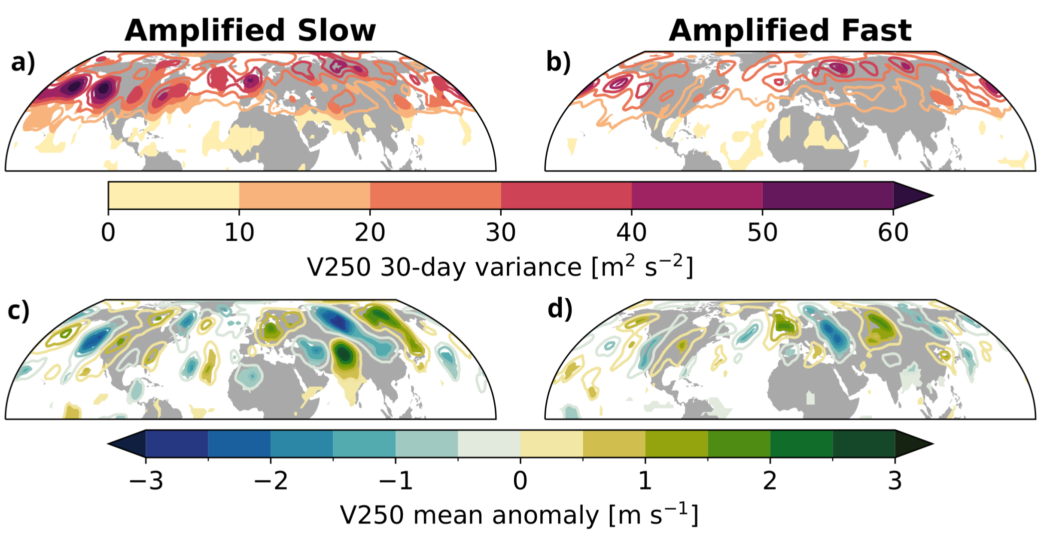

Figure 2. Variance (a, b) and mean (c, d) of 30-day mean upper-tropospheric meridional wind anomalies during for the composites as defined for Figure 1; color shading indicates a statistically significant increase in variance or a composite mean significantly different from zero at the 95% confidence level.

Motivated by the finding of a significant composite-mean signal for amplified waves with rapid phase propagation, we seek for further insight by analysing meridional wind variability at 6-hourly resolution in terms of Rossby wave packet diagnostics. In the climatological boreal summer mean (Fig. 3a, b), the Rossby wave packet envelope highlights the mid-latitude storm track of baroclinic waves maximizing over the North Pacific and North Atlantic ocean basins. Similarly, the climatological-mean phase speed maximizes in the location of the strong westerly jets. In addition, there is a clear latitudinal dependence with reduced or easterly phase speed on the equatorward side of our mid-latitude domain. These estimates agree well with the climatology computed by Fragkoulidis and Wirth (2020).

Assessing the composite-mean phase speed anomalies (Fig. 3d, f), the significant and zonally symmetric reduction in phase speed north of 35°N for the "amplified slow" composite compared to climatology validates our categorical phase speed estimate with a local phase speed metric. But we also note an intriguing increase in phase speed compared to climatology in the subtropics, possibly an indication of mid-latitude baroclinic waves penetrating further south. The "amplified fast" composite, on the other hand, exhibits a more uniform increase in phase speed across the Northern hemisphere. Given the composite criterion with a percentile threshold on meridional wind variance it is not surprising to see mostly positive composite-mean Rossby wave envelope anomalies (Fig. 3c, e). It is, however, visible that positive anomalies for the "amplified slow" composite are concentrated south of the climatological maximum, whereas for the "amplified fast" composite, the Rossby wave envelope is enhanced in place with the climatological maximum with a noticeable reduction over the Mediterranean region. The difference in composite-mean envelope anomalies indicates an equatorward displacement of upper-tropospheric waves during episodes of low zonal phase speed.

The initial hypothesis of this study was that a reduced upper-tropospheric phase speed would increase the frequency of persistent temperature extremes at the surface. Therefore, Figure 4 shows the composite-mean summer heatwave frequency anomalies in units of heatwave days per 30-day time window (climatological mean value $\approx$ 1.5 days/window in the Northern hemisphere). Statistically significant anomalies found across the Northern Hemisphere for both composites exhibit a zonally asymmetric structure with both increased and reduced heatwave frequencies. The similarity of the two maps of composite-mean anomalies, instead of a dominant increase in heatwave frequency for the "ampli-

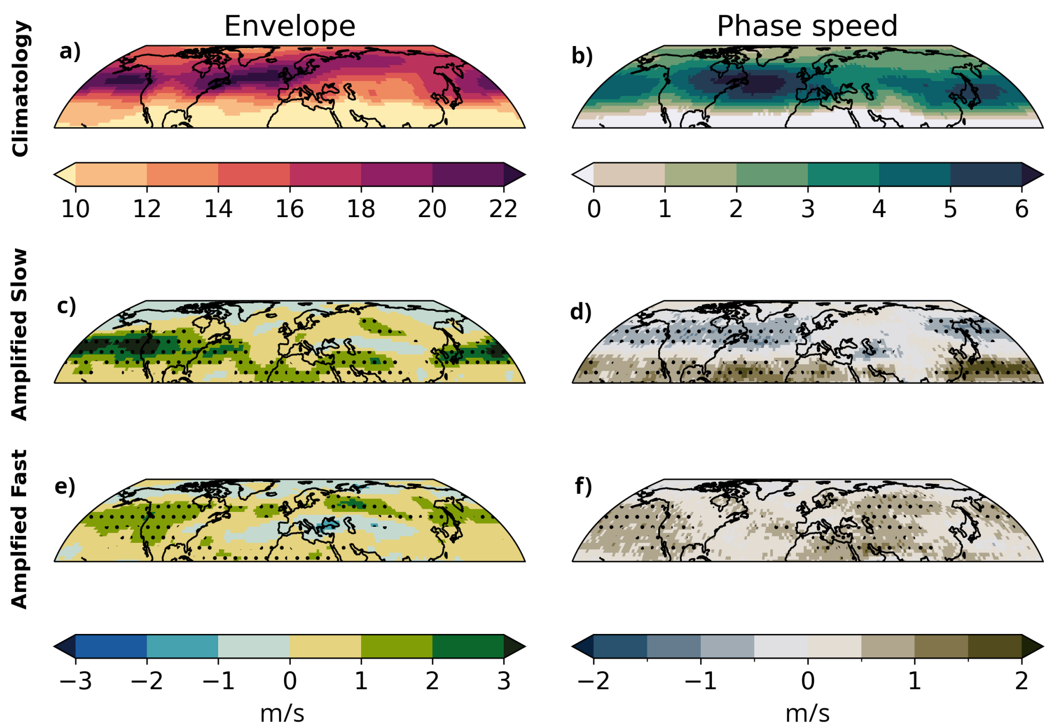

Figure 3. Climatological-mean Rossby wave packet envelope and phase speed (panel a, b) and mean anomalies (panel c, d, e, f) for composites as defined for Figure 1. Stippling indicates statistical significance at a 95% confidence level.

fied slow" composite suggested by the enhanced power of stationary waves, falsifies the initial hypothesis stated above. However, that similarity does not disprove the influence of the upper-tropospheric circulation on surface heatwave frequency.

Comparing the geographically phase-locked composite-mean wave trains (bottom row Fig. 2) with Figure 4, we find that regions of enhanced composite-mean heatwave frequency co-locate with composite-mean anticyclonic circulation anomalies. For the "amplified slow" composite, regions of enhanced heatwave frequency and anticyclonic circulation comprise, for example, the Southern United States and Western Russia, whereas Mongolia and Western Canada are highlighted in the "amplified fast" composite. The upper-tropospheric influence on surface temperature extremes in these regions is further emphasized by positive and negative anomalies in the climatological-mean heatwave duration (Fig. 4c). Specifically, the climatological-mean heatwave duration is limited to less than four days in areas where heatwave occur preferentially during episodes of rapid phase propagation, while the mean heatwave duration can exceed five days in areas that experience mean anticyclonic anomalies during episodes of slow phase propagation. This sensitivity is, however, not strong enough to produce a significant signal in the heatwave frequency.

To understand why the power of stationary waves illustrated by the composite variance of 30-day mean anomalies (Fig. 2a, b) does not exert the expected influence on heatwave frequency, two important aspects need further elaboration. First note that the relationship between the upper-tropospheric flow and surface temperature extremes is linear to such extent that a cyclonic monthly-mean anomaly reduces the likelihood of experiencing a heatwave compared to typical flow conditions. Therefore, the geographically non-phase-locked stationary waves are less effective in causing a composite-mean heatwave frequency signal than the troughs and ridges of the composite-mean wave train. Secondly, a Rossby wave packet with a typical phase speed for boreal summer is slow enough to facilitate a heatwave with minimum duration of 3 days. Therefore, the meridional shift of Rossby wave packets is more relevant for summer heatwaves than the phase speed change.

Another potential driver for mid-latitude continental heatwaves is interannual sea surface temperature variability in the form of tropical-extratropical teleconnections (e.g., Luo & Lau, 2020; Wulff et al., 2017). In particular, the negative heatwave frequency anoma-

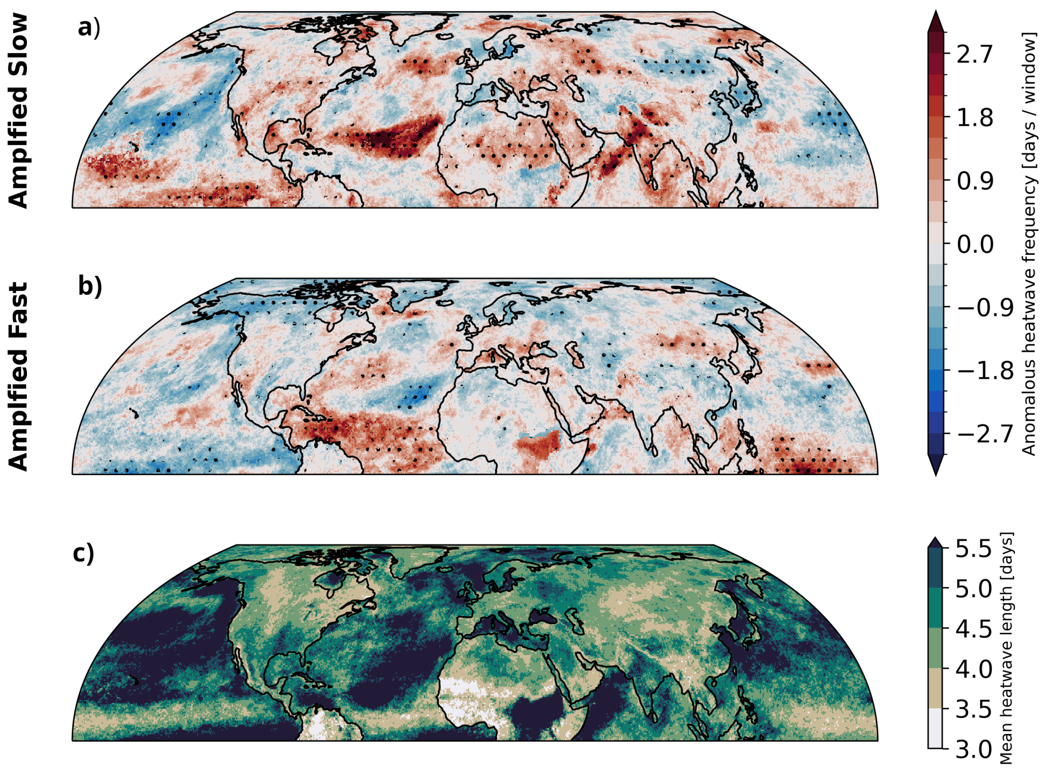

Figure 4. Mean heatwave frequency anomaly (panel a, b) for composites as defined for Figure 1 and the climatological boreal summer-mean heatwave duration (panel c). Stippling indicates a composite mean significantly different from zero at the 95% confidence level.

lies over the eastern tropical Pacific and positive anomalies over the western tropical Pacific for the "amplified fast" composite are reminiscent of sea surface temperature anomalies during the positive phase of El Niño-Southern Oscillation. This notion ties in well with the meridional shift in Rossby wave packet envelope in Figure 3 since there is a known relationship between El Niño and the extratropical storm track latitude: an equatorward storm track shift during the warm phase of El Niño has been reported over the Pacific, North America, and Europe (Fraedrich & Müller, 1992; Eichler & Higgins, 2006; Plante et al., 2015). On a similar note, the heatwave frequency anomalies over the North Atlantic for the "amplified fast" composite with a positive anomaly to the east of the United States flanked by negative anomalies to the north and south resemble the sea surface temperature tripole pattern associated with the positive phase of decadal North Atlantic Oscillation variability (e.g., Rodwell et al., 1999; Eden & Jung, 2001), another prominent mode of storm track variability.

4 Conclusions

Mid-latitude summer heatwaves are characterized as warm surface temperature extremes of a minimum duration of several days. When studying dynamical drivers, it is often assumed that persistent surface extremes require an anomalously persistent large-scale circulation in the form of amplified stationary waves (Petoukhov et al., 2013; Mann et al., 2017; Kornhuber et al., 2019; Di Capua et al., 2021). In this study, we evaluate this assumption using a categorical phase speed estimate based on spectral analysis of upper-tropospheric meridional wind. Cyclonic and anticyclonic circulation anomalies associated with the troughs and ridges of a geographically phase-locked stationary wave train cause a zonally asymmetric heatwave frequency response to changes in the phase speed of upper-tropospheric synoptic-scale waves. By shaping phase-locked stationary wave trains, phase speed is proven important for where, not whether summer heatwaves occur. An anomalously high upper-tropospheric flow persistence is, hence, not necessary for persistent warm extremes, in agreement with another recent study (Holmberg et al., 2022).

For understanding this conclusion, we highlight here that Rossby wave phase speed is a function of multiple variables. This study was designed to reduce the impact of certain covariates, for example by using a wavenumber dependant boundary between the "slow" and "fast" phase speed bin, but other covariates leave their trace in the composite-analysis. In particular, we find an equatorward shift of Rossby wave packet envelopes during episodes of slow compared to fast phase propagation. The connection between the storm track latitude and the phase speed of mid-latitude waves has previously been noted and is potentially relevant for the circulation response to climate change (Chen & Held, 2007; Shaw et al., 2016). Other covariates for phase speed variability are sea surface temperature anomalies associated with El Niño or the North Atlantic Oscillation sea surface temperature tripole.

Our phase speed estimate tailored to measure hemispheric flow persistence is well reflected in the phase speed of localized Rossby wave packets. The consequential change in mean heatwave duration compared to the global average is, however, too weak to significantly alter heatwave frequency. This raises the question about limiting factors of heatwave duration when the ridge of a wave packet is indeed stationary. Thermodynamic effects, as for example latent heat release in ascending air masses upstream of the anticyclone (Black et al., 2004; Pfahl et al., 2015; Neal et al., 2022; White et al., 2023), most likely play a role.

Open Research Section

The ERA5 reanalysis data used in this study can be downloaded from the Copernicus ClimateData Store `https://doi.org/10.24381/cds.bd0915c6`. A repository with the python code for the data analysis is available from `https://doi.org/10.5281/zenodo.10453988`.

Acknowledgments

The authors would like to thank Volkmar Wirth, Emmanuele Russo, and Andries de Vries for many fruitful discussions. This project has received funding from the European Research Council (ERC) under the European Union's Horizon 2020 research and innovation programme (grant agreement No. 847456). Support from the Swiss National Science Foundation through project PP00P2_198896 to M.P. and D.D. is gratefully acknowledged. M.P. acknowledges financial support from the Collaborative Research on Science and Society (CROSS) Program of EPFL and UNIL.

References

Ali, S. M., Martius, O., & Röthlisberger, M. (2021). Recurrent rossby wave packets modulate the persistence of dry and wet spells across the globe. *Geophysical Research Letters*, *48*(5), e2020GL091452.

Black, E., Blackburn, M., Harrison, G., Hoskins, B., Methven, J., et al. (2004). Factors contributing to the summer 2003 european heatwave. *Weather*, *59*(8), 217–223.

Chen, G., & Held, I. M. (2007). Phase speed spectra and the recent poleward shift of southern hemisphere surface westerlies. *Geophysical Research Letters*, *34*(21).

Coumou, D., Robinson, A., & Rahmstorf, S. (2013). Global increase in record-breaking monthly-mean temperatures. *Climatic Change*, *118*(3), 771–782.

Di Capua, G., Sparrow, S., Kornhuber, K., Rousi, E., Osprey, S., Wallom, D., ... Coumou, D. (2021). Drivers behind the summer 2010 wave train leading to russian heatwave and pakistan flooding. *npj Climate and Atmospheric Science*, *4*(1), 55.

Domeisen, D. I., Eltahir, E. A., Fischer, E. M., Knutti, R., Perkins-Kirkpatrick, S. E., Schär, C., ... Wernli, H. (2023). Prediction and projection of heatwaves. *Nature Reviews Earth & Environment*, *4*, 36–50. doi: https://doi.org/10.1038/s43017-022-00371-z

Ebi, K. L., Capon, A., Berry, P., Broderick, C., de Dear, R., Havenith, G., ... others (2021). Hot weather and heat extremes: health risks. *The lancet*, *398*(10301), 698–708.

Eden, C., & Jung, T. (2001). North atlantic interdecadal variability: oceanic response to the north atlantic oscillation (1865–1997). *Journal of Climate*, *14*(5), 676–691.

Eichler, T., & Higgins, W. (2006). Climatology and enso-related variability of north american extratropical cyclone activity. *Journal of Climate*, *19*(10), 2076–2093.

Fischer, E. M., & Knutti, R. (2015). Anthropogenic contribution to global occurrence of heavy-precipitation and high-temperature extremes. *Nature climate change*, *5*(6), 560–564.

Fischer, E. M., Seneviratne, S. I., Vidale, P. L., Lüthi, D., & Schär, C. (2007).

Soil moisture–atmosphere interactions during the 2003 european summer heat wave. *Journal of Climate*, *20*(20), 5081–5099.

Fraedrich, K., & Müller, K. (1992). Climate anomalies in europe associated with enso extremes. *International Journal of Climatology*, *12*(1), 25–31.

Fragkoulidis, G., & Wirth, V. (2020). Local rossby wave packet amplitude, phase speed, and group velocity: Seasonal variability and their role in temperature extremes. *Journal of Climate*, *33*(20), 8767–8787.

Fragkoulidis, G., Wirth, V., Bossmann, P., & Fink, A. (2018). Linking northern hemisphere temperature extremes to rossby wave packets. *Quarterly Journal of the Royal Meteorological Society*, *144*(711), 553–566.

García-Herrera, R., Díaz, J., Trigo, R. M., Luterbacher, J., & Fischer, E. M. (2010). A review of the european summer heat wave of 2003. *Critical Reviews in Environmental Science and Technology*, *40*(4), 267–306.

Hauser, M., Orth, R., & Seneviratne, S. I. (2016). Role of soil moisture versus recent climate change for the 2010 heat wave in western russia. *Geophysical Research Letters*, *43*(6), 2819–2826.

Hayashi, Y. (1979). A generalized method of resolving transient disturbances into standing and traveling waves by space-time spectral analysis. *Journal of Atmospheric Sciences*, *36*(6), 1017–1029.

Hersbach, H., Bell, B., Berrisford, P., Hirahara, S., Horányi, A., Muñoz-Sabater, J., ... others (2020). The era5 global reanalysis. *Quarterly Journal of the Royal Meteorological Society*, *146*(730), 1999–2049.

Holmberg, E., Messori, G., Caballero, R., & Faranda, D. (2022). The counter-intuitive link between european heatwaves and atmospheric persistence. *Earth System Dynamics Discussions*, 1–26.

Jiménez-Esteve, B., & Domeisen, D. I. (2022). The role of atmospheric dynamics and large-scale topography in driving heatwaves. *Quarterly Journal of the Royal Meteorological Society*, *148*(746), 2344–2367.

Jiménez-Esteve, B., Kornhuber, K., & Domeisen, D. (2022). Heat extremes driven by amplification of phase-locked circumglobal waves forced by topography in an idealized atmospheric model. *Geophysical Research Letters*, *49*(21), e2021GL096337.

Kornhuber, K., Osprey, S., Coumou, D., Petri, S., Petoukhov, V., Rahmstorf, S., &

Gray, L. (2019). Extreme weather events in early summer 2018 connected by a recurrent hemispheric wave-7 pattern. *Environmental Research Letters*, *14*(5), 054002.

Luo, M., & Lau, N.-C. (2020). Summer heat extremes in northern continents linked to developing enso events. *Environmental Research Letters*, *15*(7), 074042.

Mann, M. E., Rahmstorf, S., Kornhuber, K., Steinman, B. A., Miller, S. K., & Coumou, D. (2017). Influence of anthropogenic climate change on planetary wave resonance and extreme weather events. *Scientific reports*, *7*(1), 1–12.

Meehl, G. A., & Tebaldi, C. (2004). More intense, more frequent, and longer lasting heat waves in the 21st century. *Science*, *305*(5686), 994–997.

Miralles, D. G., Teuling, A. J., Van Heerwaarden, C. C., & Vilà-Guerau de Arellano, J. (2014). Mega-heatwave temperatures due to combined soil desiccation and atmospheric heat accumulation. *Nature geoscience*, *7*(5), 345–349.

Neal, E., Huang, C. S., & Nakamura, N. (2022). The 2021 pacific northwest heat wave and associated blocking: meteorology and the role of an upstream cyclone as a diabatic source of wave activity. *Geophysical Research Letters*, *49*(8), e2021GL097699.

Petoukhov, V., Rahmstorf, S., Petri, S., & Schellnhuber, H. J. (2013). Quasiresonant amplification of planetary waves and recent northern hemisphere weather extremes. *Proceedings of the National Academy of Sciences*, *110*(14), 5336–5341.

Pfahl, S., Schwierz, C., Croci-Maspoli, M., Grams, C. M., & Wernli, H. (2015). Importance of latent heat release in ascending air streams for atmospheric blocking. *Nature Geoscience*, *8*(8), 610–614.

Pfahl, S., & Wernli, H. (2012). Quantifying the relevance of atmospheric blocking for co-located temperature extremes in the northern hemisphere on (sub-) daily time scales. *Geophysical Research Letters*, *39*(12).

Plante, M., Son, S.-W., Atallah, E., Gyakum, J., & Grise, K. (2015). Extratropical cyclone climatology across eastern canada. *International Journal of Climatology*, *35*(10), 2759–2776.

Randel, W. J., & Held, I. M. (1991). Phase speed spectra of transient eddy fluxes and critical layer absorption. *Journal of the atmospheric sciences*, *48*(5), 688–697.

Riboldi, J., Lott, F., d'Andrea, F., & Rivière, G. (2020). On the linkage between rossby wave phase speed, atmospheric blocking, and arctic amplification. *Geophysical Research Letters*, *47*(19), e2020GL087796.

Rodwell, M. J., Rowell, D. P., & Folland, C. K. (1999). Oceanic forcing of the wintertime north atlantic oscillation and european climate. *Nature*, *398*(6725), 320–323.

Rossby, C.-G. (1945). On the propagation of frequencies and energy in certain types of oceanic and atmospheric waves. *Journal of the Atmospheric Sciences*, *2*(4), 187–204.

Röthlisberger, M., Frossard, L., Bosart, L. F., Keyser, D., & Martius, O. (2019). Recurrent synoptic-scale rossby wave patterns and their effect on the persistence of cold and hot spells. *Journal of Climate*, *32*(11), 3207–3226.

Röthlisberger, M., Pfahl, S., & Martius, O. (2016). Regional-scale jet waviness modulates the occurrence of midlatitude weather extremes. *Geophysical Research Letters*, *43*(20), 10–989.

Russo, E., & Domeisen, D. I. (2023). Increasing intensity of extreme heatwaves: the crucial role of metrics. *Geophysical Research Letters*, *50*(14), e2023GL103540.

Russo, S., Sillmann, J., & Fischer, E. M. (2015). Top ten european heatwaves since 1950 and their occurrence in the coming decades. *Environmental Research Letters*, *10*(12), 124003.

Schneidereit, A., Schubert, S., Vargin, P., Lunkeit, F., Zhu, X., Peters, D. H., & Fraedrich, K. (2012). Large-scale flow and the long-lasting blocking high over russia: Summer 2010. *Monthly Weather Review*, *140*(9), 2967–2981.

Shaw, T., Baldwin, M., Barnes, E. A., Caballero, R., Garfinkel, C., Hwang, Y.-T., ... others (2016). Storm track processes and the opposing influences of climate change. *Nature Geoscience*, *9*(9), 656–664.

Simmons, A. J., & Hoskins, B. J. (1979). The downstream and upstream development of unstable baroclinic waves. *Journal of the Atmospheric Sciences*, *36*(7), 1239–1254.

Sousa, P. M., Trigo, R. M., Barriopedro, D., Soares, P. M., & Santos, J. A. (2018). European temperature responses to blocking and ridge regional patterns. *Climate Dynamics*, *50*, 457–477.

White, R. H., Anderson, S., Booth, J. F., Braich, G., Draeger, C., Fei, C., ... others (2023). The unprecedented pacific northwest heatwave of june 2021. *Nature*

Communications, *14* (1), 727.

White, R. H., Kornhuber, K., Martius, O., & Wirth, V. (2022). From atmospheric waves to heatwaves: A waveguide perspective for understanding and predicting concurrent, persistent, and extreme extratropical weather. *Bulletin of the American Meteorological Society*, *103* (3), E923–E935.

Wirth, V. (2020). Waveguidability of idealized midlatitude jets and the limitations of ray tracing theory. *Weather and Climate Dynamics*, *1* (1), 111–125.

Wirth, V., & Polster, C. (2021). The problem of diagnosing jet waveguidability in the presence of large-amplitude eddies. *Journal of the Atmospheric Sciences*, *78* (10), 3137–3151.

Wirth, V., Riemer, M., Chang, E. K., & Martius, O. (2018). Rossby wave packets on the midlatitude waveguide—a review. *Monthly Weather Review*, *146* (7), 1965–2001.

Wulff, C. O., Greatbatch, R. J., Domeisen, D. I., Gollan, G., & Hansen, F. (2017). Tropical forcing of the summer east atlantic pattern. *Geophysical Research Letters*, *44* (21), 11–166.

Yeh, T.-c. (1949). On energy dispersion in the atmosphere. *Journal of Atmospheric Sciences*, *6* (1), 1–16.

Yiou, P., Cattiaux, J., Faranda, D., Kadygrov, N., Jézéquel, A., Naveau, P., … others (2020). Analyses of the northern european summer heatwave of 2018. *Bulletin of the American Meteorological Society*, *101* (1), S35–S40.

Zimin, A. V., Szunyogh, I., Patil, D., Hunt, B. R., & Ott, E. (2003). Extracting envelopes of rossby wave packets. *Monthly weather review*, *131* (5), 1011–1017.

Zschenderlein, P., Fragkoulidis, G., Fink, A. H., & Wirth, V. (2018). Large-scale rossby wave and synoptic-scale dynamic analyses of the unusually late 2016 heatwave over europe. *Weather*, *73* (9), 275–283.

Figure 1.

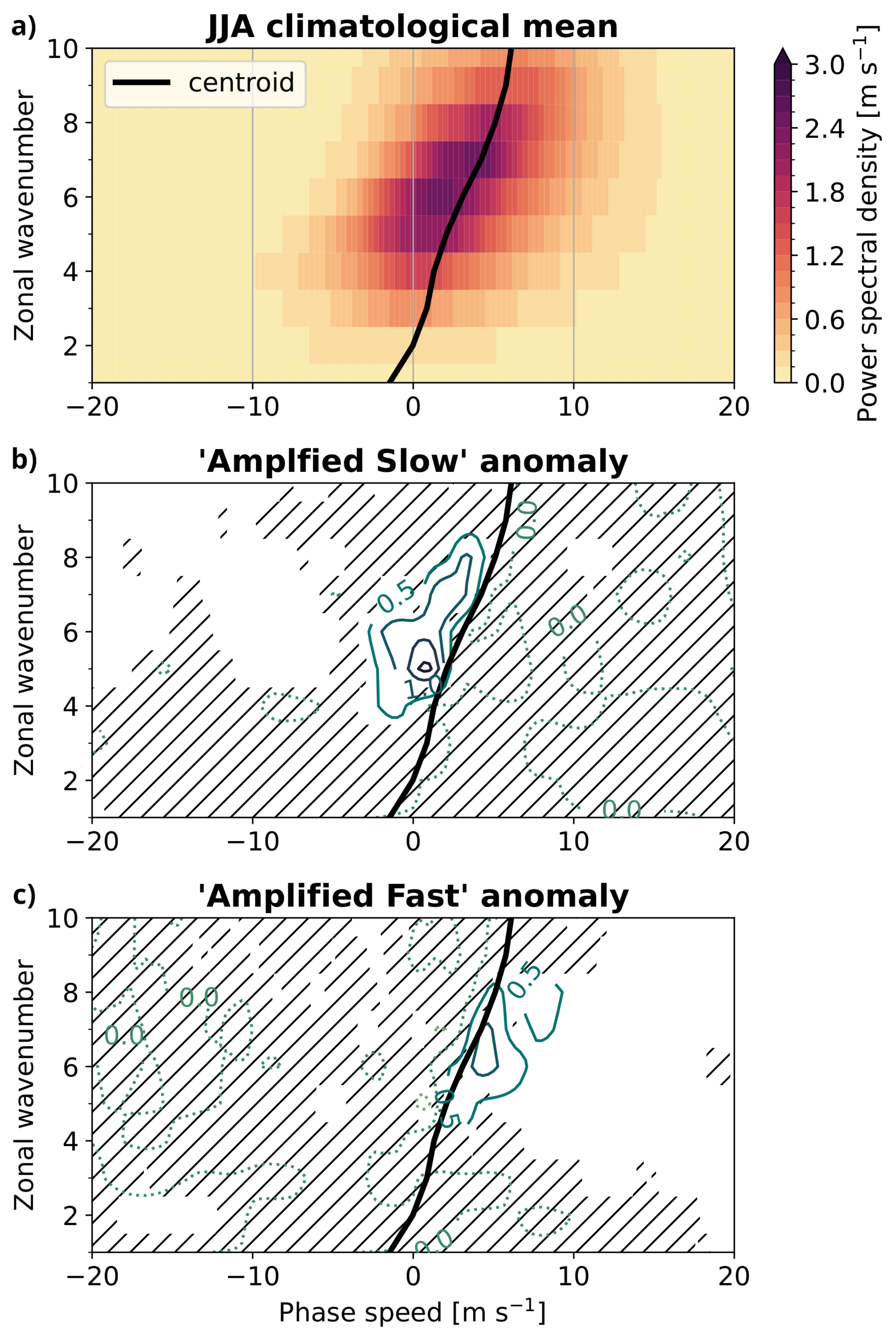

a)
JJA climatological mean
centroid
Zonal wavenumber
Power spectral density [m s^{-1}]
3.0
2.4
1.8
1.2
0.6
0.0
b)
'Amplfied Slow' anomaly
0.5
1.0
0.0
c)
'Amplified Fast' anomaly
0.5
0.0
Phase speed [m s^{-1}]

Figure 2.

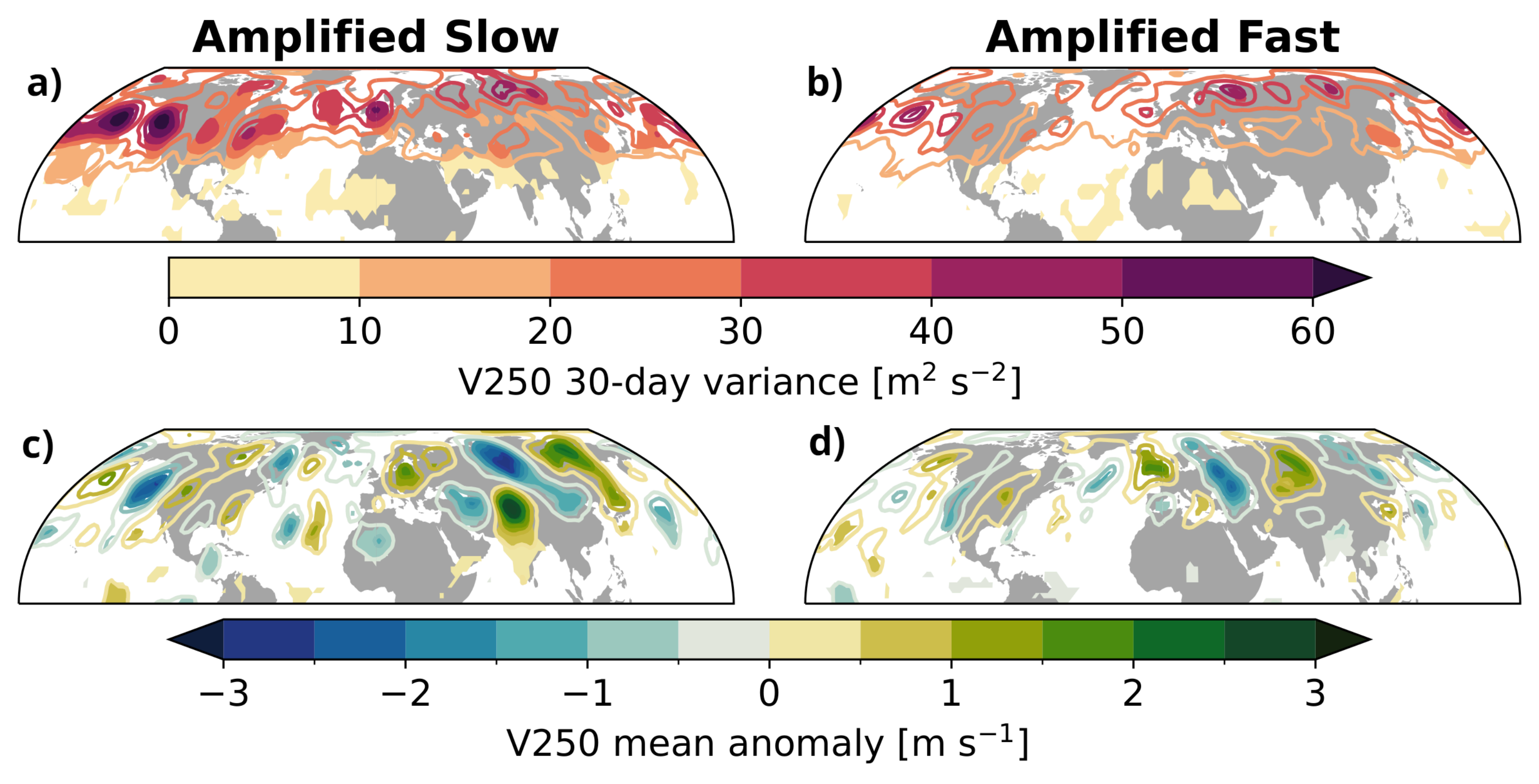

Amplified Slow
Amplified Fast
a)
b)
0
10
20
30
40
50
60
V250 30-day variance [m^2 s^{-2}]
c)
d)
−3
−2
−1
0
1
2
3
V250 mean anomaly [m s^{-1}]

Figure 3.

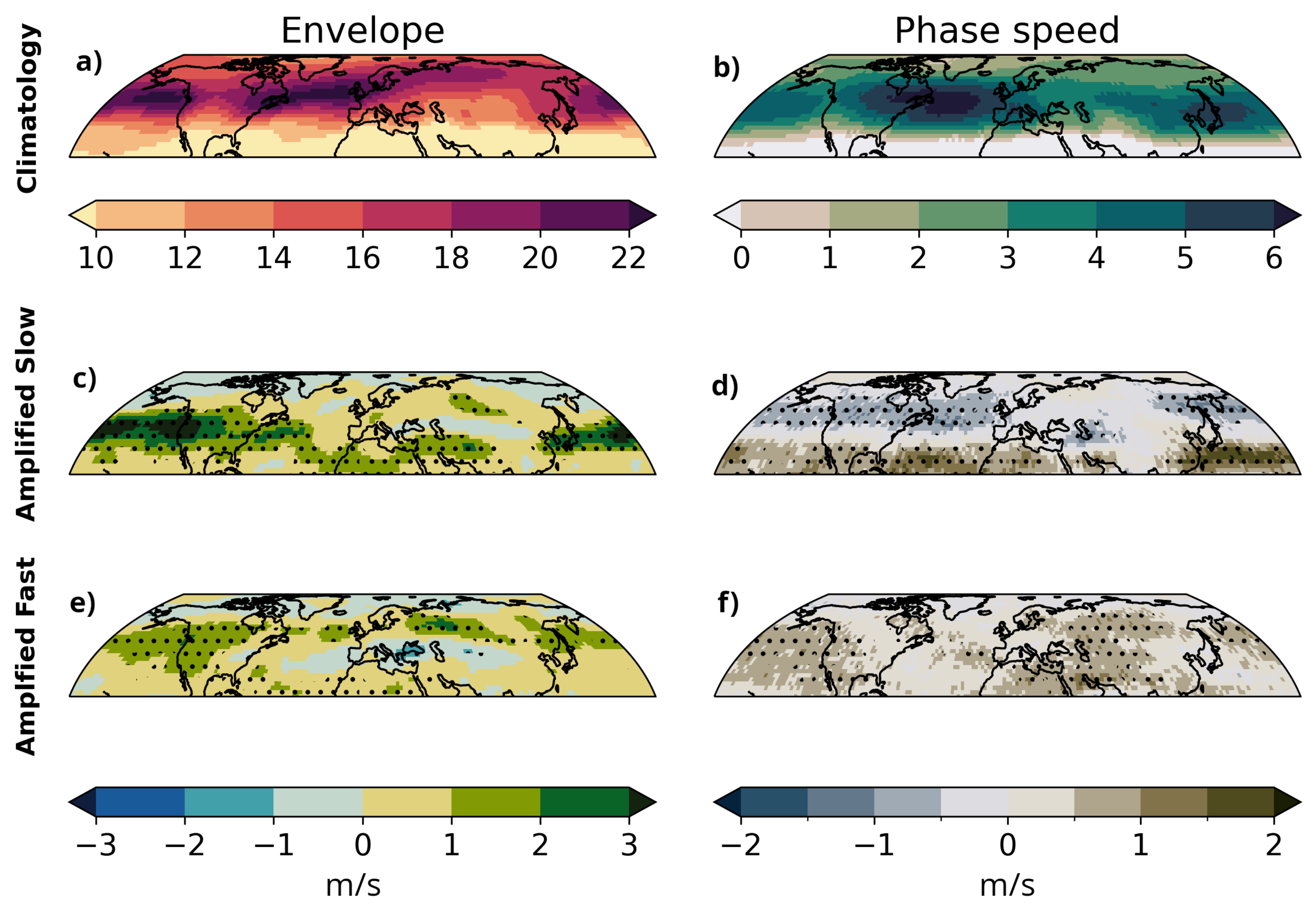
Envelope
Phase speed
Climatology
Amplified Slow
Amplfied Fast
a)
b)
c)
d)
e)
f)
10
12
14
16
18
20
22
0
1
2
3
4
5
6
−3
−2
−1
0
1
2
3
m/s
−2
−1
0
1
2
m/s

Figure 4.

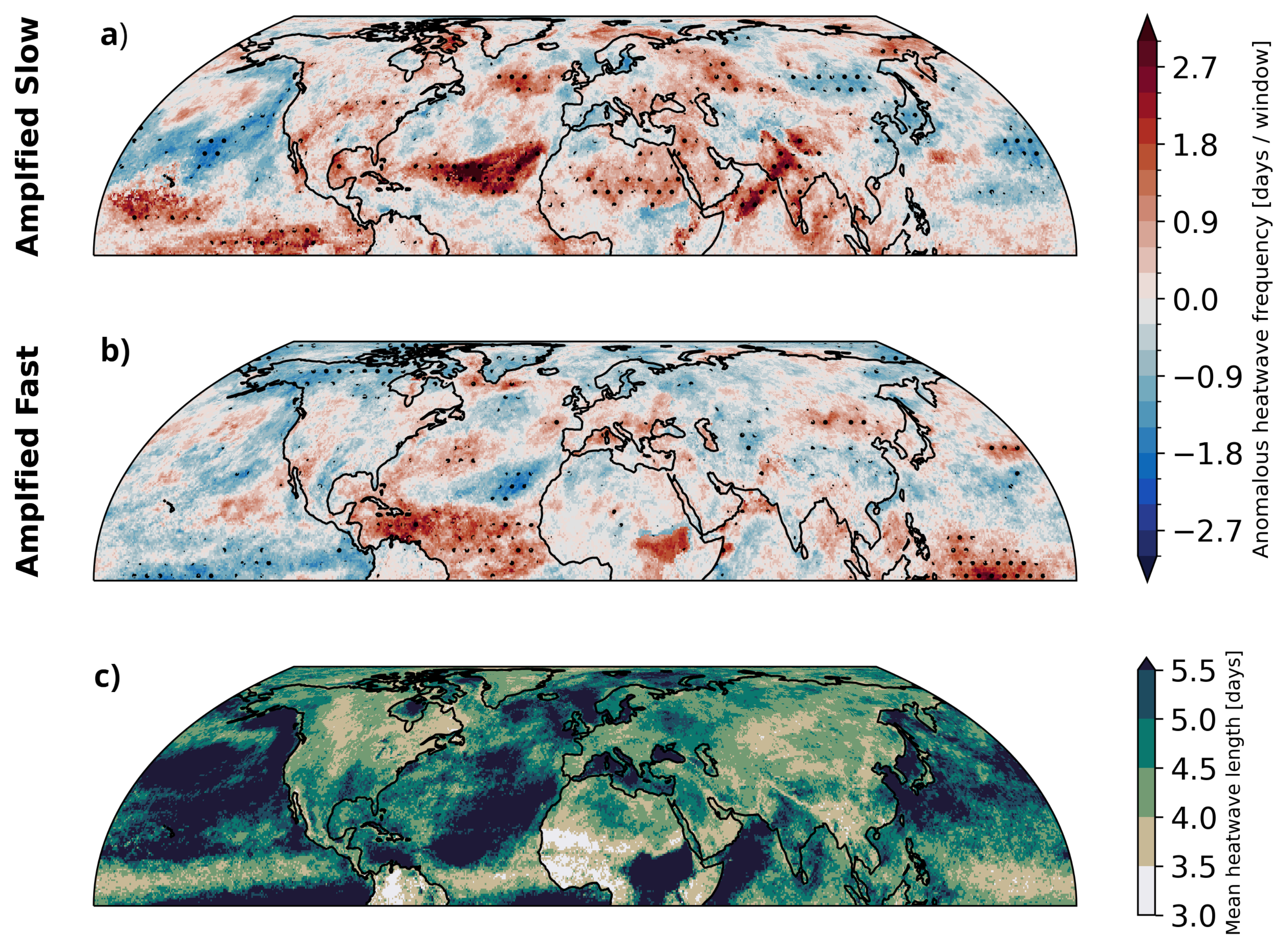

a)
b)
c)
Amplfied Slow
Amplfied Fast
Anomalous heatwave frequency [days / window]
2.7
1.8
0.9
0.0
−0.9
−1.8
−2.7
Mean heatwave length [days]
5.5
5.0
4.5
4.0
3.5
3.0

Supporting Information for "Rossby Wave Phase Speed Influences Heatwave Location through a Shift in Storm Track Position"

Wolfgang Wicker[1], Nili Harnik[2], Maria Pyrina[3], Daniela I. V. Domeisen[1,3]

[1]Faculty of Geosciences and Environment, University of Lausanne, Lausanne, Switzerland

[2]Porter School of the Environment and Earth Sciences, Tel Aviv University, Tel Aviv, Israel

[3]Department of Environmental Systems Science, ETH Zurich, Zurich, Switzerland

Contents of this file

Introduction

The main manuscript introduces a categorical phase speed estimate based on spectral analysis. Technical details about the two-dimensional Fourier transform and the choice of the 30-day window length are presented in Text S1 and Figure S1. The analysis that follows in the main manuscript uses a composite criterion on meridional wind variance

---

Corresponding author: W. Wicker, Institute of Earth Surface Dynamics, University of Lausanne, Géopolis – UNIL Mouline, 1015 Lausanne, Switzerland. (wolfgang.wicker@unil.ch)

aggregated for zonal wavenumbers 5-8. The results are qualitatively similar when focusing on individual wavenumbers as shown in Figure S2. In order to very briefly address potential waveguideability aspects, Figure S3 depicts a composite analysis of zonal wind anomalies.

Text S1.

The Fourier coefficients $B_{k,\omega}$ with zonal wavenumber $k \geq 0$ and angular frequency ω for the transformation of gridded meridional wind anomalies $v_{m,n}$ with M time steps Δt and N points in longitude are given by

$$B_{k,\omega} = \frac{\sqrt{2\Delta t}}{N\sqrt{M}} \sum_{m=0}^{M-1} \sum_{n=0}^{N-1} v_{m,n} e^{-i[\omega m \Delta t + 2\pi k n/N]} \tag{1}$$

Power spectral density ρ_{k,c_p} at latitude ϕ and phase speed $c_p = a\cos\phi(\omega/k)$, where a denotes the Earth's radius, can be computed as

$$\rho_{k,c_p} = B_{k,\omega} B^*_{k,\omega} \frac{k}{2\pi a \cos\phi} \tag{2}$$

The centroid C_k of a phase speed spectrum is defined as

$$C_k = \sum^{S} \rho_{k,c_p} c_p \Big/ \sum^{S} \rho_{k,c_p} \tag{3}$$

The time series of extratropical meridional wind variance V_k in the respective phase speed bin S are obtained by integration of power spectral density ρ_{k,c_p} using the centroid C_k as the lower bound for the "fast" and the upper bound for the "slow" phase speed bin. The correlation of meridional wind variance between the two phase speed bins is sensitive to the time window length used for the Fourier transformation of meridional wind anomalies (Fig. S1). As stated in the main manuscript, a 30-day window is chosen to obtain two time series that are uncorrelated while maintaining a sufficiently large sample size. For shorter windows, the reduced phase speed resolution results in a positive correlation of meridional wind variance, whereas for longer windows the spectra suffer from increased noisiness. The resulting correlation coefficients, shown in bold letters on the main diagonal of the upper right and lower left quadrant of Figure S1, are close to zero and statistically insignificant. A positive correlation for adjacent wavenumbers in the same phase speed bin is the signature of localized Rossby wave packets. The statistical significance of these correlation coefficients is indicated by the red shading of the boxes next to the main diagonal of Figure S1 and caused by spectral leakage during the Fourier transformation along the zonal dimension.

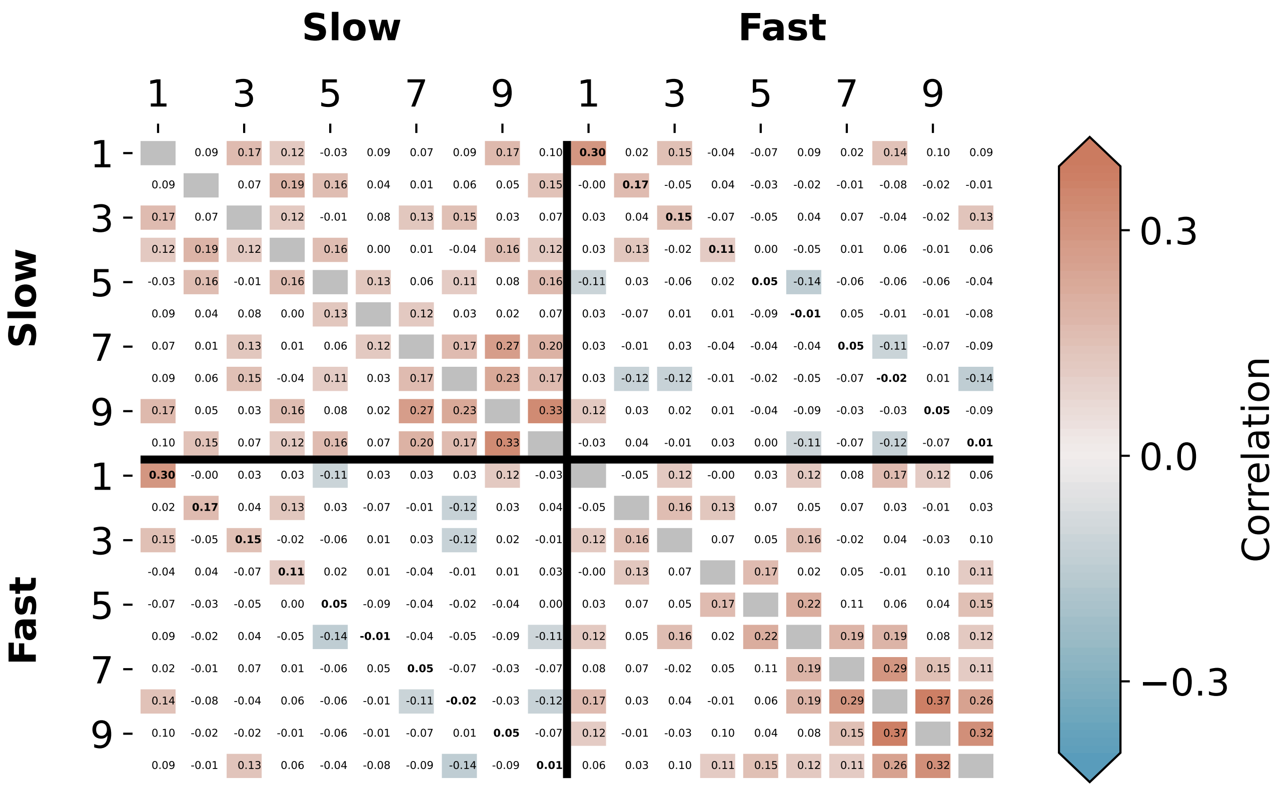

Figure S1. Pearson correlation coefficients between time series of meridional wind variance for different zonal wavenumbers in the 'slow' and 'fast' phase speed bins, respectively, color shaded where statistically significant at the 95% confidence level.

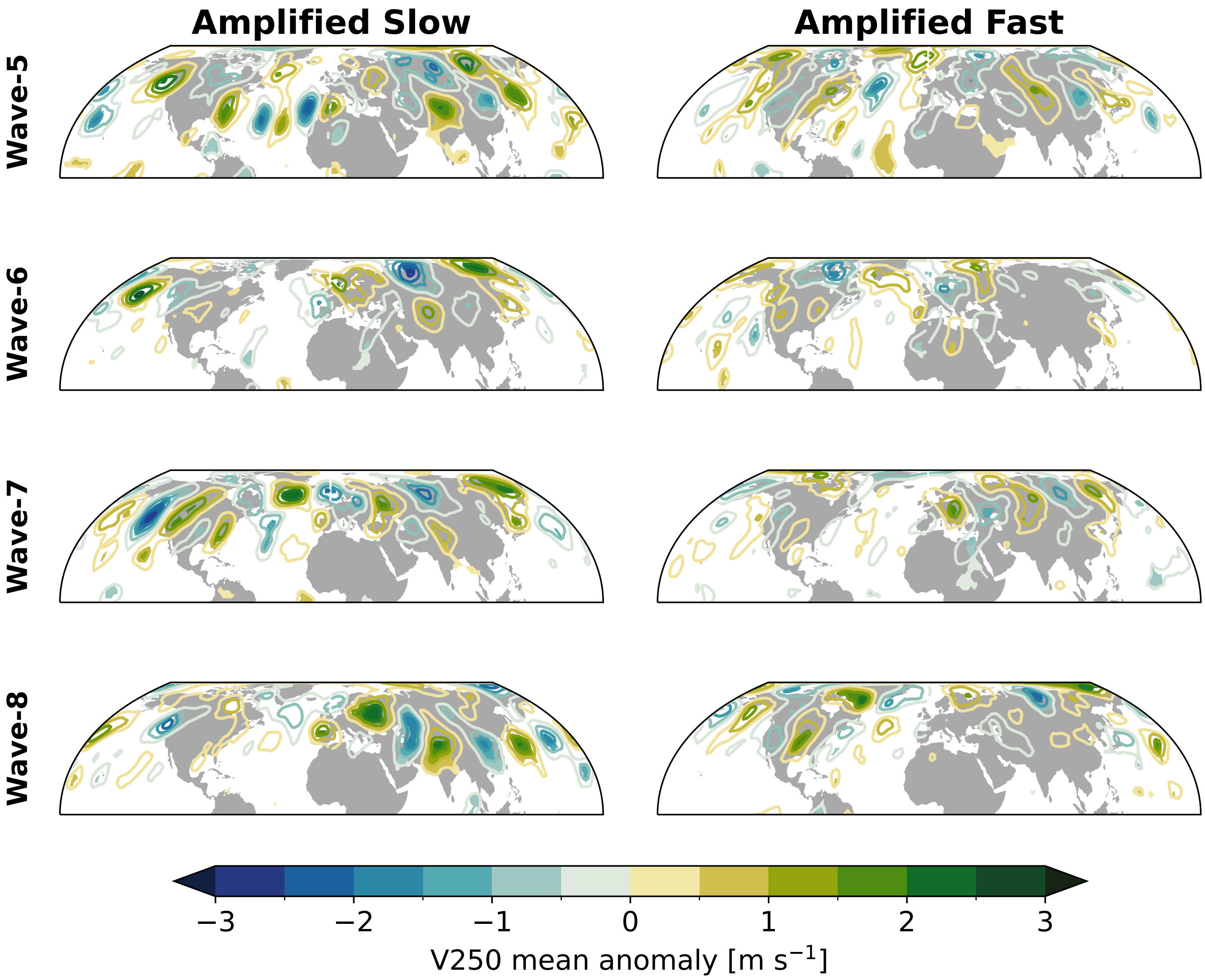

Figure S2. Composite mean of 30-day mean upper-tropospheric meridional wind anomalies during episodes when the meridional wind variance for individual zonal wavenumbers exceeds the 90th percentile in the respective phase speed bin; color shading indicates a statistically significant increase in variance or a composite mean significantly different from zero at the 95% confidence level.

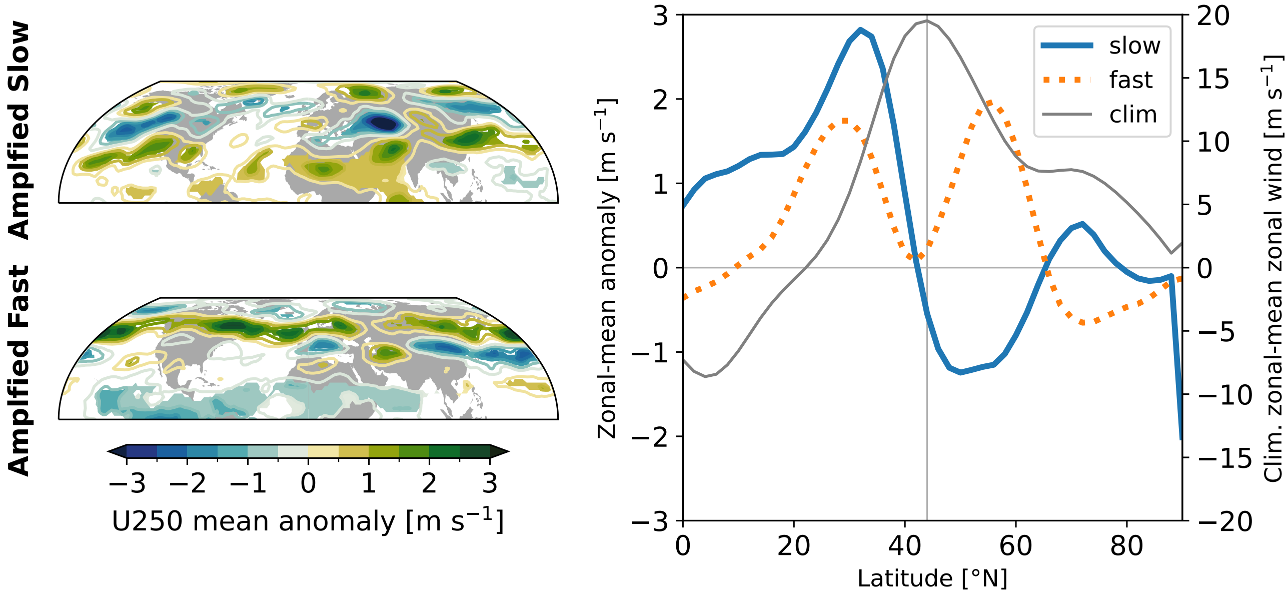

Figure S3. Composite mean of 30-day mean upper tropospheric wind anomalies as in Figure 2 but for zonal wind (left column), as well as, zonal-mean zonal wind climatology and zonal-mean composite-mean anomalies at 250hPa (right column). Note that the horizontal maps use a sub-seaonally varying climatology whereas the zonal-mean anomalies are computed with respect to a fixed JJA mean.